Techno-economic study of compound parabolic collector in solar water heating system in the northern hemisphere

Hooman Azad Gilani[a] and Siamak Hoseinzadeh[b],*

[a]Department of Mechanical Engineering, Eastern Mediterranean University, G. Magosa, TRNC Mersin 10, Turkey
[b]Centre for Asset Integrity Management, Department of Mechanical and Aeronautical Engineering, University of Pretoria, Pretoria, South Africa

*Corresponding author. Hosseinzadeh.siamak@up.ac.za; Hoseinzadeh.siamak@gmail.com

Highlights

• CPC and FPC energy and cost savings are comparatively investigated.
• Twenty locations with different solar radiations and energy costs are considered.
• Yearly solar radiations range from 2509 to 852 kWh/m^2.
• Yearly savings in auxiliary heating rates vary from 27% to 5%.
• In locations with high energy price CPC is economically feasible
.

Abstract

The auxiliary requirement of a solar water heating system is an index of the end-user's cost and, thus, the feasibility of the system. Within this study several locations worldwide with high and low solar radiations and electricity prices in latitudes of 0, 15, 30, 45 and 60°N have been selected and the effect of employing a Compound Parabolic Collector (CPC) on the yearly auxiliary energy saving of a solar water heating system has been investigated numerically and compared with the energy performance of a typical flat plat collector. The yearly solar radiation in selected locations ranges from 2509 to 852 kWh/m^2. Electricity prices also vary from 0.04 to 0.28 USD/kWh. According to results, in all selected locations, CPC shows an advantage over flat plate collectors in auxiliary power consumption. The yearly auxiliary heating rate decreased maximum by 27% in Shambat in Sudan and minimum by 5% in Chongqing in China. As solar radiation increases, the advantage of CPC becomes more meaningful. Regarding costs and economic feasibility of CPC, maximum net present values are all achieved in the locations with the highest electricity prices and not very high discount rates. Selected locations in Japan and Italy with maximum NPV values of 1,981 and 1,811 UDS, respectively, have the highest electricity rates of 0.28 and 0.27 USD/kWh, in respect. In both countries, the discount rate is relatively low and about 0.3. Moreover, among the selected locations, NPV of investment on CPC in Gabon, Guatemala, USA, Japan and Sweden with low levels of solar radiation, between 974 and 1,942 kWh/m^2, is between 832 and 1,981 USD at the end of the project's life time and justifies the employment of this type of solar collector in sites with high energy prices, even though not much solar radiation is available. It could be concluded that in locations with high electricity prices and not very much discount rates, even in cases of relatively low solar radiation, investment in CPC would yield the highest profits.

Keywords: Solar energy; Water heating; Compound parabolic collector; Flat plate collector; Thermoeconomic analysis

Nomenclature

A_a	Aperture area m^2	(TA)	Overall transmittance-absorbtance product –
A_r	Receiver area m^2	α	Short-wave absorptance of the absorber plate –
A_{ref}	Reflector area m^2	α_{eff}	effective absorptance –
C	Concentration ratio –	β	Collector tilt angle °
C_L	Specific heat J/kg K	γ	Surface azimuth angle °
F_b	Control function –	γ_s	Solar azimuth angle °
F_R	Collector heat removal factor –	η	Collector efficiency –
F_{gnd}	View factor to the ground –	θ	Incident angle for beam radiation °
F_{sky}	View factor to the sky –	θ_1	The angle of incidence °
F'	Collector efficiency factor –	θ_2	The angle of refraction °
I	Rate of total solar radiation on a horizontal surface W/m^2	θ_c	Half-acceptance angle °
I_{bT}	Rate of solar beam radiation on a tilted surface W/m^2	θ_d	Diffuse effective incidence angle °
I_d	Rate of solar diffuse radiation on a horizontal surface W/m^2	θ_t	Transverse acceptance angle °
I_T	Rate of total solar radiation on a tilted surface W/m^2	θ_z	Zenith angle °
K	Extinction coefficient m^{-1}	ρ_{eff}	Effective reflectance of the reflector –
L	Cover thickness m	ρ_d	Effective reflectance of the reflector –
$\dot{m}$	Mass flow rate Kg/s	ρ_g	Ground reflectance –
n_g	Refractive index –	ρ_R	The reflectivity of the CPC walls –
n_r	An average number of reflections –	$\rho_\perp$	Reflectance perpendicular component of polarization –
$\dot{Q}_{loss}$	Collector's total heat loss W	$\rho_\parallel$	Reflectance parallel component of polarization –
$\dot{Q}_u$	Rate of useful solar energy gain of a collector W	τ	The transmittance of cover –
$r_\perp$	The perpendicular component of reflection of unpolarized radiation	τ_a	Transmittance with only absorption losses has been considered –
$r_\parallel$	Parallel component of reflection of unpolarized radiation –	$\tau_\perp$	Transmittance perpendicular component of polarization –
U_L	Collector overall heat loss coefficient W/m^2 K	$\tau_\parallel$	Transmittance parallel component of polarization –
U_{tank}	Thermal energy of the tank J	$(\tau\alpha)$	Product of the cover transmittance and the absorber absorptance –

s	Absorber width m	$(\tau\alpha)_b$	$(\tau\alpha)$ for beam radiation (depends on the incidence angle θ) –
T_a	Ambient temperature °C	$(\tau\alpha)_d$	$(\tau\alpha)$ for sky diffuse radiation –
T_r	Absorber temperature °C	$(\tau\alpha)_g$	$(\tau\alpha)$ for ground reflected radiation –
T_i	Collector inlet temperature °C	$(\tau\alpha)_n$	$(\tau\alpha)$ at normal incidence –

1. Introduction

No solar water heating system can rely solely on solar heat gain to meet the heating loads. Hence, an auxiliary energy source is an essential part of every solar water heating system. This auxiliary heating requirement is a decisive criterion for the feasibility of solar water heating systems for meeting-related thermal loads in a particular location. Flat plate collectors are widely used for water heating systems. High efficiency, low cost, and easy installation and maintenance are among the reasons for the popularity of flat plate collectors. However, incorporating other types of more efficient solar collectors in water heating applications could increase energy savings and environmental impacts. One of the potential designs to increase the efficiency of solar collectors is using the concentration concept.

Compound Parabolic Collectors (CPCs) are one of the promising concentrating solar collectors for domestic hot water applications since they can produce high-temperature water even when sun rays do not strike the collector at an optimized angle, meaning they can be implemented without a tracking system. This reason makes CPC a potential candidate as a more efficient solar collector for low-temperature applications. The key differences between CPC and flat plate collector could be summarized as following:

- CPC employs the concentration concept and for the same aperture area, less absorber area is required and so less heat loss accrues from the absorber.
- •Concentrating solar radiation on a smaller absorber area makes it possible for CPC to archive higher outlet temperatures, compared with a flat plate collector.
- •Flat plate collectors are used in low-temperature applications while concentrating collectors are usually used in medium or high-temperature applications.
- •CPC can capture sun rays at relatively smaller incident angles compared with flat plat collectors.

The purpose of this study is to investigate, based on the end user's cost, under what conditions CPC is most profitable economically. To accomplish this, the northern hemisphere is chosen since it accommodates the majority of the world's population, and all the locations with available meteorological data in latitudes of 0, 15, 30, 45, and 60° are chosen to demonstrate how increasing the latitude may affect the comparative performance of the two collectors. Among these locations, the ones with the highest and lowest radiations and electricity prices are detected, and then the locations with the combinations of highest radiation-highest energy price, highest radiation-lowest energy price, lowest radiation-highest energy price, and lowest radiation-lowest energy price are selected. The yearly auxiliary

heating rates of a solar water heating system with a flat plate collector and a CPC are calculated and compared. Then a feasibility study regarding the profitability of using CPC in each location is presented. Such a comprehensive worldwide research on the thermal performance and auxiliary energy-saving and economic benefits of a water heating system with a CPC is not available in the literature. Thus the present study provides beneficial insight into the potential benefits of utilizing a CPC in water heating applications. The study uses a CPC with design, configuration, and dimensions similar to real commercial CPCs available in the market. This is another feature of the current study. Finally, the study presents comprehensive details of TRNSYS formulations and procedures for calculating the thermal performance of a CPC. The authors used this formulation to develop a MATLAB code and generated results that were in agreement with TRNSYS within less than 1% error. Therefore, other researchers may quickly and readily use the provided formulation to develop their codes and accomplish their numerical studies.

2. Background

Compound parabolic collectors (CPC) are non-imaging concentrating collectors which can provide concentration without tracking the sun. CPC was invented by Hsieh [1] and Winston [2] described the principle and geometry of a two dimensional CPC for the first time. Since then, many papers have been published regarding the design and analysis of CPC. Some of this research is documented in [3], [4], [5], [6], [7], [8], [9], [10], [11], [12], [13], [14], [15], [16], [17], [18], [19], [20], [21]. Moreover, researches have tried continuously to devise methods to improve the efficiency of this kind of solar collector, which in the following, some of them will be reviewed. Some researches indicate that under the same testing conditions, the heat losses from flat plate collectors are up to 32% higher compared to a CPC [22]. CPCs can reach temperatures in the range of 250 °C and are simple and reliable in design and operation [23]. Dielectric CPC is used to enlarge the acceptance angle of a CPC for the same geometry. In this type of CPC, the collector is filled with a dielectric material. The law of refraction implies that by increasing the refractive index of the dielectric, the maximum values of both internal and external acceptance angles for a dielectric-filled CPC, under total internal reflection conditions at certain refractive indices, will increase [24]. For dielectric-filled CPC, materials like clear polyurethane [25], [26], PMMA (polymethyl methacrylate) also called acrylic [27], borosilicate glass [28] and other common optical materials in useful visible and infrared region are applicable, as the dielectrics depend on the requirements of refractive index.

Different geometries for the absorber have been investigated. A prototype performance of 2D trough CPC with a flat absorber on base was examined by Al-Ghasem, et al. [29]. Mishra, et al. [30] integrated the U-shaped evacuated tabular collector with a compound parabolic concentrator to optimize the evacuated tabular collector. Ratismith, et al. [31] devised two innovative CPCs, both having a double-sided absorber plate in the middle. One is a double-parabolic trough and the other is a flat-base trough. The performance of four CPC collectors with different absorbers (one horizontal cylinder, two horizontal cylinders placed side by side, two horizontal cylinders one placed on the other and one horizontal oval) was compared [32], [33].

Several types of research have been done regarding CPC and solar water heating systems. An overview of various types of solar-assisted water heating systems, including the one with CPC, and their market potential is presented in [34]. An Integrated Collector Storage (ICS) solar water heater was designed, constructed and studied by [35]. An advanced mathematical

model capable of simulating the energy performance of an innovative Integrated Collector Storage Solar Water Heater (ICSSWHs) is presented by Smyth, et al. [36]. Brottier and Bennacer [37] performed a statistical study to analyze in-field performances of twenty-eight hybrid solar domestic hot water installations equipped with innovative non-overglazed PVT collectors in Western Europe (France, Switzerland and Portugal). An experiment with a CPC-type solar water heater system with a U-pipe was set up by Gang, et al. [38], and its performance in meeting higher temperature requirements was investigated. [39] presents up to date developments in integrated collector storage solar water heater using CPC. A parametric study of a concentrating integrated collector storage solar water heater was undertaken by Varghese and Manjunath [20]. A CPC was built and used as the concentrator. By Experimental measurements, data was collected to obtain correlations for a monthly solar fraction of the system. The Energy-saving of the solar system, compared with a system with no solar collector, was estimated by using f-chart method and EES software. Based on energy-saving, the return of investment was estimated. In another study, the thermal performances of six integrated collector storage systems (ICS) with different acceptance angels were compared, two of which incorporated a CPC and four with involute reflectors [40]. NING, et al. [41] installed a CPC heat pipe coupled vacuum tube solar water heater and an all-glass evacuated tube solar water heater and tested them at the same working conditions. Techno-economic analysis of an integrated collector storage solar water heater with CPC reflector for households is provided by Varghese, et al. [42].

Although CPCs have received a lot of attention from researchers in recent years, not too much information is available on the long term performance of CPC in low-temperature water heating applications. The question of under which conditions utilizing a CPC for a solar water heating system is beneficial has not been addressed in the literature. This research investigates this issue in a very wide scope to fulfill these gaps. To do so, the annual auxiliary power consumption of a solar water heating system, which is of economical and environmental interest, has been compared for cases of utilizing a CPC and a flat plate collector. The study includes twenty locations with low and high solar radiations and electricity prices in the northern hemisphere. An economical cost analysis follows the energy comparison to determine in what conditions the CPC application could be most profitable economically.

3. Thermal performance of CPC

There are several models to describe the thermal performance of a CPC mathematically. In this section, the mathematical formulation of the CPC component (type75) in TRNSYS is reviewed in full detail [43]. Calculating the thermal performance of a CPC could be divided into three steps, as discussed in this section. TRNSYS models a CPC with a flat absorber The three steps are as follows:

3.1. Calculating the average number of internal reflections (optical model)

Using the X-Y coordinates, like the ones shown in Fig. 1, the equation of a branch of CPC could be written as:

$$Y = \frac{X^2}{2s(1+\sin\theta_c)} \tag{1}$$

which θ_c and s are the collector's half-acceptance angle and absorber's width, respectively. The X-coordinate of the endpoint of the branch is:

$$X_s = s\cos\theta_c \tag{2}$$

and

$$\overline{X} = s\left[\frac{1+\sin\theta_c}{\cos\theta_c}\right]\left[-\sin\theta_c + (1+\frac{\overline{h}}{h}\cot^2\theta_c)^{1/2}\right] \tag{3}$$

which h is the height of the full CPC and $\overline{X}$ and $\overline{h}$ are shown in Fig. 1. The concentration ratio of the CPC is found by:

$$C = \frac{A_a}{A_r} = 2\left(\frac{\overline{X}}{s}\right)\cos\theta_c - \left(\frac{\overline{X}}{s}\right)^2\frac{\sin\theta_c}{\sin\theta_c+1} + \sin\theta_c - \cos^2\theta_c \tag{4}$$

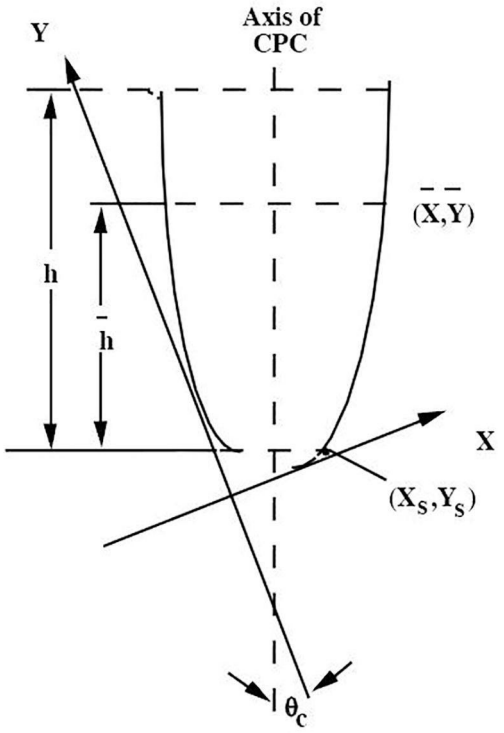

Fig. 1. X-Y Coordinates Used in the Formulation of the Compound Parabolic Collector [43].

For a full CPC, $\overline{h}/h = 1$, the concentration ratio is $1/\sin\theta_c$. The concentration ratio falls off by truncating the CPC.

n_r , the average number of internal reflections, could be expressed as:

$$n_r = \frac{A_{ref}}{A_r}\left(\frac{1}{2} - \frac{\overline{X}^2 - X_s^2}{2A_{ref}s(1+\sin\theta_c)}\right) \tag{5}$$

A_{ref} is the reflector's area and is found by

$$\frac{A_{ref}}{A_r} = (1+\sin\theta_c)\, ln\left[\frac{\frac{\overline{X}}{s}+\sqrt{(1+\sin\theta_c)^2+\left(\frac{\overline{X}}{s}\right)^2}}{\cos\theta_c+\sqrt{2(1+\sin\theta_c)}}\right]+\frac{\overline{X}}{s}\sqrt{1+\left(\frac{\overline{X}}{s(1+\sin\theta_c)}\right)^2} - \frac{\cos\theta_c\sqrt{2}}{\sqrt{1+\sin\theta_c}} \quad (6)$$

3.2. Calculating the transmittance-absorbance products

TRNSYS uses the TALF subroutine to calculate transmittance-absorbance products for beam, diffuse, and ground reflected radiations [43]. For more information on the related equations, mathematical reference of TRNSYS documentation or chapter 5 of [44] could be consulted counsulted. The procedure for calculating transmittance-absorbance products is as follows:

Fresnel's equations for reflectance at a planar interface for perpendicular and parallel unpolarized radiation are:

$$r_\perp = \frac{\sin^2(\theta_1-\theta_2)}{\sin^2(\theta_1+\theta_2)} \quad (7)$$

$$r_\parallel = \frac{ta\,n^2(\theta_1-\theta_2)}{\tan^2(\theta_1+\theta_2)} \quad (8)$$

θ_1 and θ_2 are related by Snell's Law:

$$\sin\theta_1 = n_g \sin\theta_2 \quad (9)$$

where the index of fraction for air is taken unity.

Allowing for both reflection and absorption losses, cover transmittance perpendicular and parallel components of polarization are:

$$\tau_\perp = \frac{\tau_a(1-r_\perp)^2}{1-(r_\perp\tau_a)^2} \quad (10)$$

$$\tau_\parallel = \frac{\tau_a(1-r_\parallel)^2}{1-(r_\parallel\tau_a)^2} \quad (11)$$

Which τ_a is the transmittance when only absorption losses have been considered:

$$\tau_a = \exp\left(-\frac{KL}{\cos\theta_2}\right) \quad (12)$$

To find the cover transmittance, the transmittances for the parallel and perpendicular components of polarization are averaged:

$$\tau = \frac{1}{2}(\tau_\perp+\tau_\parallel) = \frac{\tau_a}{2}\left[\frac{(1-r_\perp)^2}{1-(r_\perp\tau_a)^2}+\frac{(1-r_\parallel)^2}{1-(r_\parallel\tau_a)^2}\right] \quad (13)$$

Similarly, for reflectance, perpendicular and parallel components of polarization are:

$$\rho_{\perp} = r_{\perp}\left(1 + \tau_a \tau_{\perp}\right) \tag{14}$$

$$\rho_{\parallel} = r_{\parallel}\left(1 + \tau_a \tau_{\parallel}\right) \tag{15}$$

And reflectance of the cover again is found by averaging these components:

$$\rho = \tfrac{1}{2}(\rho_{\perp} + \rho_{\parallel}) = \tfrac{1}{2}\left[r_{\perp}\left(1 + \tau_a \tau_{\perp}\right) + r_{\parallel}\left(1 + \tau_a \tau_{\parallel}\right)\right] \tag{16}$$

Finally, the transmittance-absorptance product is calculated by:

$$(\tau\alpha) = \frac{\tau\alpha_{eff}}{1-(1-\alpha_{eff})\rho_d} \tag{17}$$

ρ_d , the reflectance of the cover for diffuse radiation incident coming from the absorber surface, is obtained by using (16) at the diffuse effective incidence angle, θ_d , which is given by:

$$\theta_d = \theta_g = 44.86 - 0.0716\theta_c + 0.00512\theta_c^2 - 0.00002798\theta_c^3 \tag{18}$$

All transmittance-absorbance products are determined using an effective absorbance:

$$\alpha_{eff} = \rho_{eff}\alpha \tag{19}$$

where $\rho_{eff} \approx \rho_R^{n_r}$, in which ρ_R is the wall reflectance and is the average number of internal reflections, given by (5).

$(\tau\alpha)_d = (\tau\alpha)_g$ are calculated at diffuse and ground reflected effective incidence angles in which $\theta_d = \theta_g$, and θ_d is given by (18).

3.3. Calculating the useful solar heat gain

The CPC absorber is modeled using the Hottel-Whillier model collector such that:

$$\dot{Q}_u = A_a F_R \left[I_T\,(\mathrm{TA}) - U_L\,(T_i - T_a)\right] \tag{20}$$

which U_L is the overall loss coefficient per unit aperture area and F_R is the collector heat removal factor and is given by:

$$F_R = \frac{\dot{m}C_p}{A_a U_L}\left[1 - \exp\left(-\frac{A_a U_L F'}{\dot{m}C_p}\right)\right] \tag{21}$$

And the overall transmittance-absorbtance product, (TA), is calculated as:

$$(\mathrm{TA}) = \frac{(\tau\alpha)_b F_b I_{bT} + (\tau\alpha)_d I_d F_{sky} + (\tau\alpha)_g \rho_g I F_{gnd}}{I_T} \quad (22)$$

View factors to the sky and ground are used to estimated diffuse radiation entering the aperture. For the transverse receiver orientation:

$$F_{sky} = \frac{1/C + \min(1/C, \cos\beta)}{2} \quad (23)$$

$$F_{gnd} = \frac{\max(1/C, \cos\beta) - \cos\beta}{2} \quad (24)$$

Both beam and diffuse radiations could be collected by CPC when approaching the aperture within a critical angle of a half-acceptance angle θ_c .

In this simulation, the CPC receiver has been located in a transverse plane 90° from the longitudinal orientation. In this case, beam radiation enters the CPC when $\theta_t < \theta_c$ where:

$$\theta_t = \tan^{-1}\left(\frac{\sin\theta_z \sin(\gamma - \gamma_s)}{\cos\theta}\right) \quad (25)$$

In (22) F_b is a control function so that $F_b = 1$ if the sun is within the acceptance angle, let's say $\theta_t < \theta_c$, and $F_b = 0$ otherwise.

By definition, efficiency, η , of a CPC is the ratio of the rate of useful solar energy gain of the collector to the rate of total incident radiation on the aperture plane, that is:

$$\eta = \frac{\dot{Q}_u}{A_a I_T} \quad (26)$$

3.4. The calculation procedure in MATLAB

The authors used the formulation presented in sections 3.1 to 3.3 to develop a MATLAB code and calculated the value of 754.26 kWh for the yearly useful solar heat gain of the CPC in Zahedan in Iran. This value was in agreement with the TRNSYS value of 761.11 kWh with a 0.9% error. The procedure of calculation is shown in Fig. 2. The input weather data includes hourly values of the total and sky diffuse radiations on horizontal, total radiation on a tilted surface, solar azimuth and zenith angles, angle of incidence for tilted surface, and ambient temperature. All these hourly values could be exported from Type109-TMY2 in TRNSYS as separate txt files. The fopen command in MATLAB reads the input data.

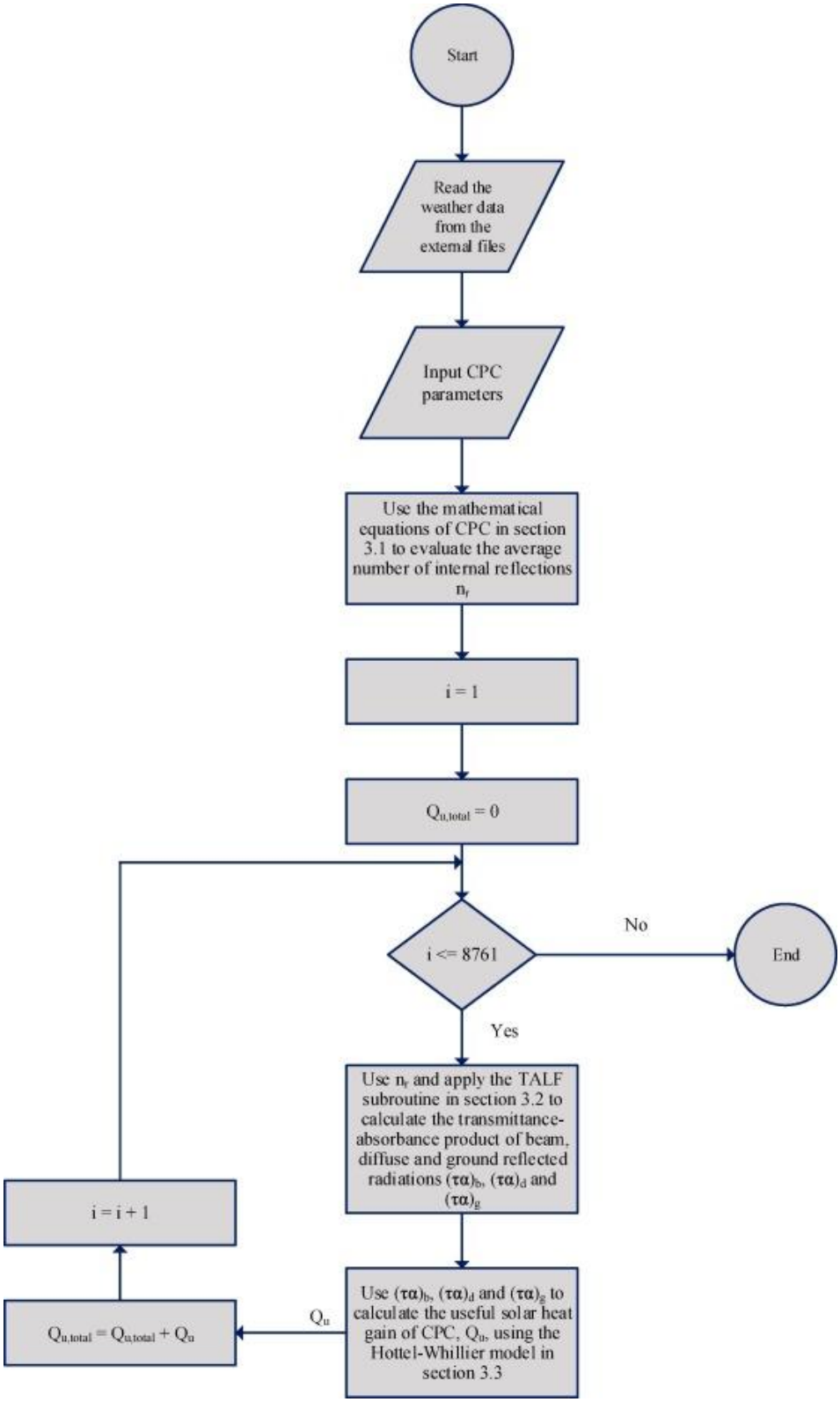

Fig. 2. The Procedure of Calculating the Yearly Useful Solar Heat Gain of a CPC.

The calculations in the loop's body are done with the hourly weather data to evaluate the hourly values of useful solar heat gain. The results of each subsection of Section 3 are used as an input for the next subsection. In Section 3.1, the average number of internal reflections is calculated. In Section 3.2, is used to calculate transmittance-absorbance products , and.

Finally, in Section 3.3, all transmittance-absorbance products are used by the Hottel-Whillier model to calculate the useful solar heat gain. The total yearly solar heat gain is calculated by summing the hourly values of each of the 8760 hours of the year.

4. Numerical study

4.1. Modeling

A schematic of a simple solar water heating system is shown in Fig. 3. A flat plate collector and a CPC with a flat absorber have been used as the collector of the system, alternatively. A daily water usage profile like the one suggested by Klein [45] and shown in Fig. 4 is used. Daily hot water consumption of 120 L (or 119.64 kg) at 60 °C for a family of four (30L/person) is assumed. Also, it is assumed that the mains water enters the tank at 15 °C. The auxiliary heater is controlled such that if the temperature of the water of the tank is less than 60 °C, it will heat the water from the storage tank temperature to 60 °C. A dead band temperature difference of 5 °C is set. This makes the electric element start heating the water when the temperature sensor at the top of the storage tank reads a temperature 5 °C below the setpoint temperature.

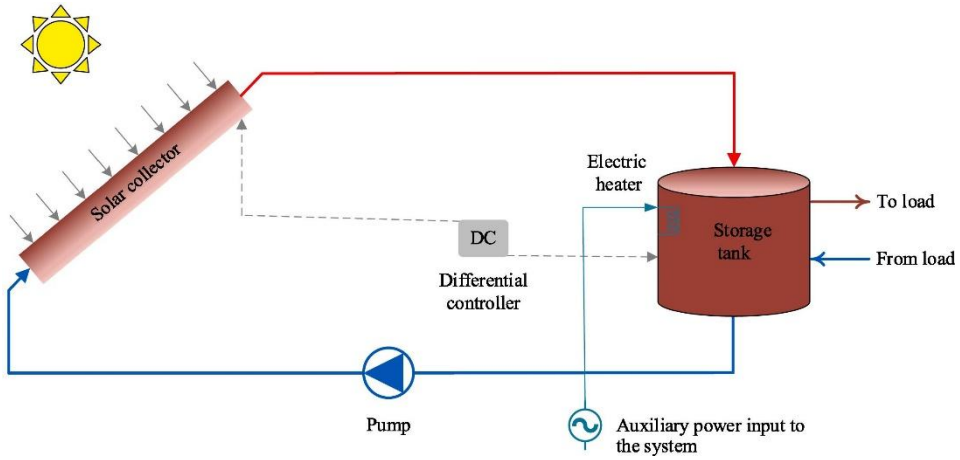

Fig. 3. A Typical Solar Water Heating System.

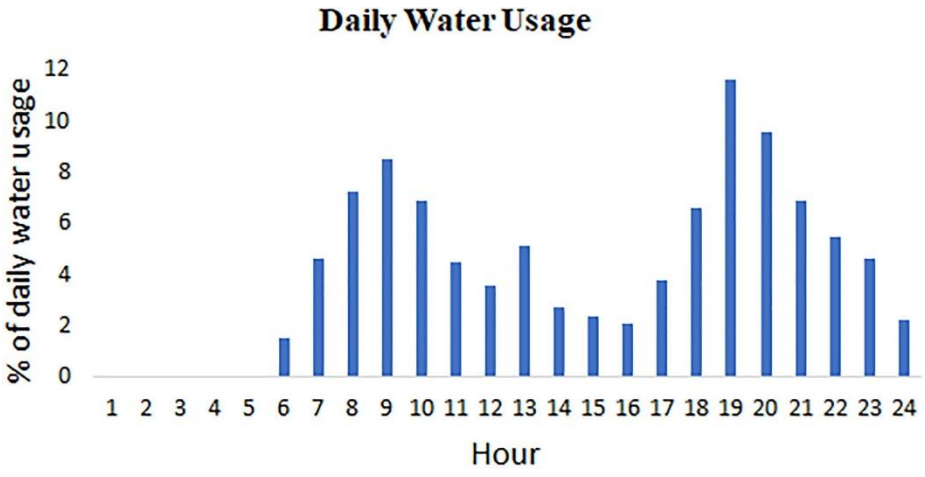

Fig. 4. Daily Water Usage Profile [45]

The auxiliary heating rates of the system with both collectors are calculated and used to calculate and compare the energy costs for the end-user. Table 1, Table 2, Table 3 list the parameters used in the simulation. The parameters of the two collectors are taken identical as much as possible to investigate the effects of the parabolic reflectors on the thermal performance of the CPC. The apertures have an area of 2 m^2 with 1 m width and 2 m length. The CPC consists of five small CPCs with equal aperture areas and inlet flowrates, connected in parallel. Using the assumed parameters given in Table 1, the dimensions of each small CPC have been calculated and listed in Table 4. The symbols refer to Fig. 1. Fig. 5 shows a 2-D drawing of one small CPC with the related dimensions. Fig. 6 shows a 3-D drawing of the five small CPC reflectors connected in parallel. The collector's slope is equal to the latitude of the installation site. To preserve the consistency with the mathematical formulation of the thermal performance of CPC, the isotropic sky model has been used as the sky model for diffuse radiation calculations. First, yearly performances of the systems in Zahedan in Iran at the low latitude of 30°N and with a high yearly solar radiation value of 2,509 kWh and Kingisepp in Russia at the high latitude of 60°N and with a low yearly solar radiation value of 908 kWh are reviewed in detail. Next, in latitudes of 0, 15, 30, 45, and 60°, among the 383 locations with available weather data, the locations with the highest and lowest yearly available solar radiation and electricity price are identified. For each latitude, four combinations as locations with the highest radiation-highest price, highest radiation-lowest price, lowest radiation-highest price, and lowest radiation-lowest price are identified and selected (Fig. 7). The yearly performances of the system with a flat plate collector (FPC) and a CPC are calculated and compared for these twenty selected locations. In the end, a feasibility study regarding the costs and financial profitability of using CPC instead of FPC in selected locations will be provided.

Table 1. Parameters of each CPC.

Parameter	Value
Collector area (m^2)	0.4
Fluid specific heat (J/kg K)	4190
Collector fin efficiency factor (–)	0.94
Overall heat loss coefficient (W/m^2 K)	3.3
Collector wall reflectivity (–)	0.9
Collector half-acceptance angle (–)	60
Truncation ratio (–)	0.5425
Absorptance of absorber plate (–)	0.9
Axis orientation	Transverse
Inlet flowrate (kg/s)	0.00556

Table 2. Flat plate collector parameters.

Parameter	Value
Collector area (m^2)	2
Fluid specific heat (J/kg K)	4190
Collector fin efficiency factor (–)	0.94
Bottom, edge loss coefficient ()	0.45
Absorber plate emittance (–)	0.95
Absorptance of absorber plate (–)	0.9
Inlet flowrate (kg/s)	0.0278

Table 3. Storage tank parameters.

Parameter	Value
Storage tank capacity per collector area (kg/m^2)	75
Tank Volume (m^3)	0.15
Tank heat loss coefficient (W/m^2 °C)	0.8
Setpoint temperature (°C)	60
Dead band for the heating element (°C)	5

Table 4. Dimensions of each CPC.

Parameter	Symbol	Value
Aperture area (m^2)	A_a	0.4
Half-acceptance angle (m)	θ_c	60
Truncation ratio (–)	$\frac{\bar{h}}{h}$	0.5425
Aperture width (m)	L	0.2
Concentration ratio (–)	C	1.125
Absorber width (m)	s	0.1778
Height (m)	$\bar{h}$	0.06

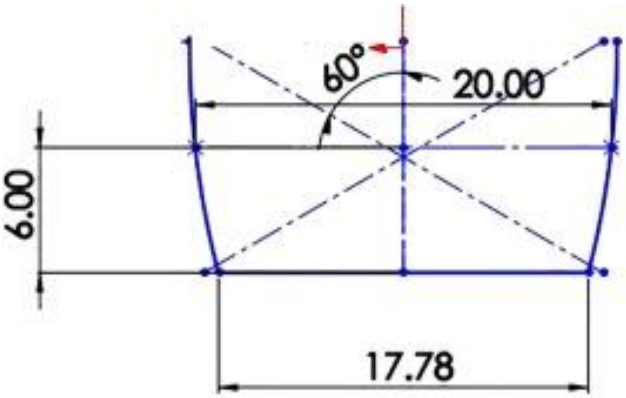

Fig. 5. 2-D Drawing of Each CPC (Dimensions Are in cm).

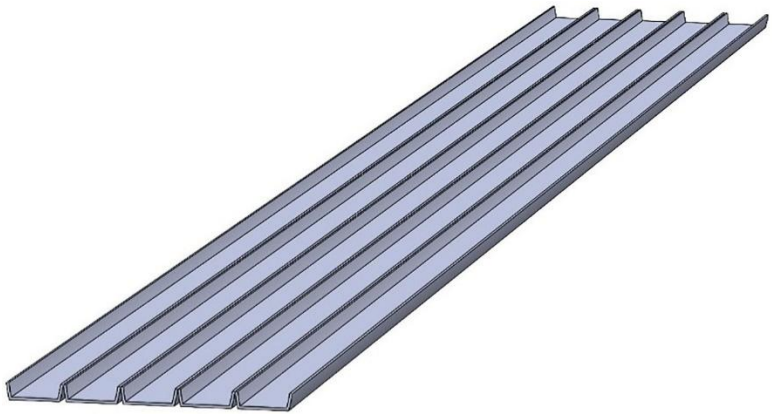

Fig. 6. 3-D Drawing of the Truncated CPC Reflectors.

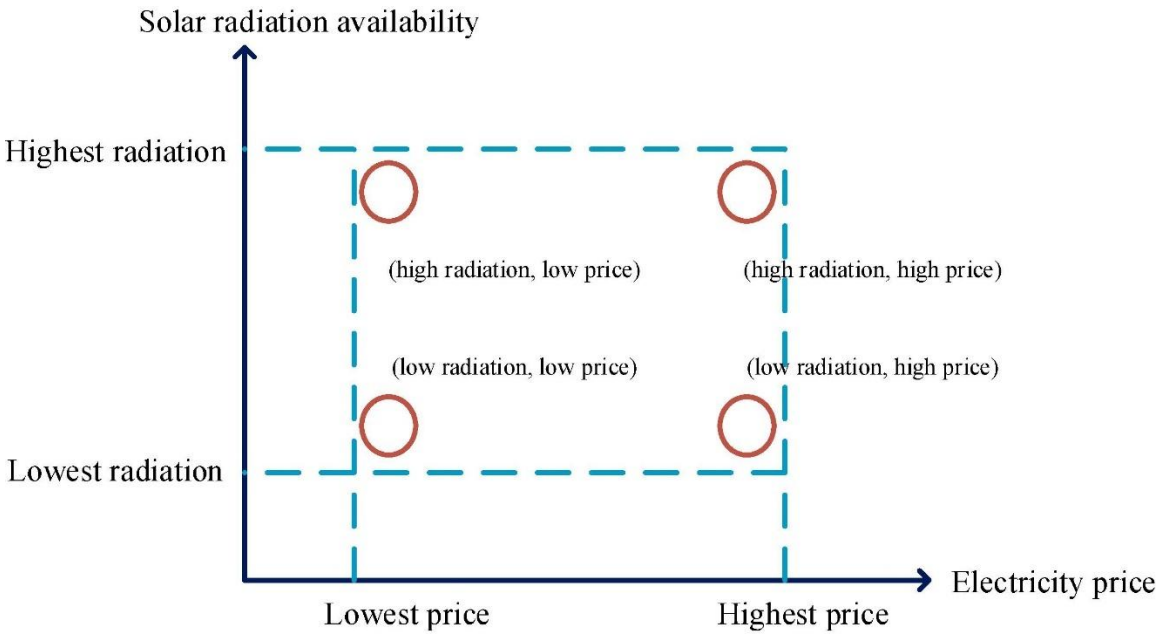

Fig. 7. Combinations of Solar Radiation Availabilities and Electricity Prices in Selected Locations.

4.2. Limitations of TRNSYS

There are some remarks needed to be considered. TRNSYS takes the overall heat loss coefficient of the CPC as a constant parameter, defined by the user. However, as is the case for flat plate collectors, the overall heat loss coefficient of a CPC strongly depends on temperature. In concentrating collectors, due to higher temperatures, the dependence of the loss coefficient on temperature is more important and assuming the overall heat loss coefficient as a constant parameter is not a realistic assumption. To carry more accurate numerical studies on CPCs, either empirical correlations for overall heat loss coefficient as a function of temperature should be developed and used in (20), or more fundamentally, might be obtained through iteration by applying heat balance on the absorber and cover to find the absorber temperature and total heat loss, and then evaluate by:

$$\dot{Q}_{loss} = A_r U_L \left(T_r - T_a\right) \tag{27}$$

A method for accomplishing the latter approach has been presented by Rabl [46].

5. Results and discussion

5.1. Energy savings

Fig. 8 shows the monthly average values of solar radiation on the collector surface in Zahedan and Kingisepp. Relatively high solar radiation levels, mostly beam radiation, strike the collector’s surface in Zahedan throughout the year. Much lower total and beam radiations are available in Kingisepp. The average hourly efficiency, Eta, and the cumulative efficiency, Eta_total, of both collectors for Zahedan and Kingisepp are shown in Fig. 9. In both locations, CPC provides higher efficiencies. However, in Kingisepp, during winter, the collectors operate with very low efficiencies. Fig. 10 shows the hourly average collector temperatures at noon. It is observed that, while in both locations, CPC provides higher temperatures compared with FPC, the advantage of CPC over FPC in Zahedan is more meaningful. In Kingisepp, for both collectors, only during the middle months of the year, the collector's average outlet temperature exceeds the average inlet temperature. It means that in winter, there is not enough solar radiation available to heat the water. Thus, the collector’s pump is not working, and no data is available for the collector’s outlet temperatures in these months.

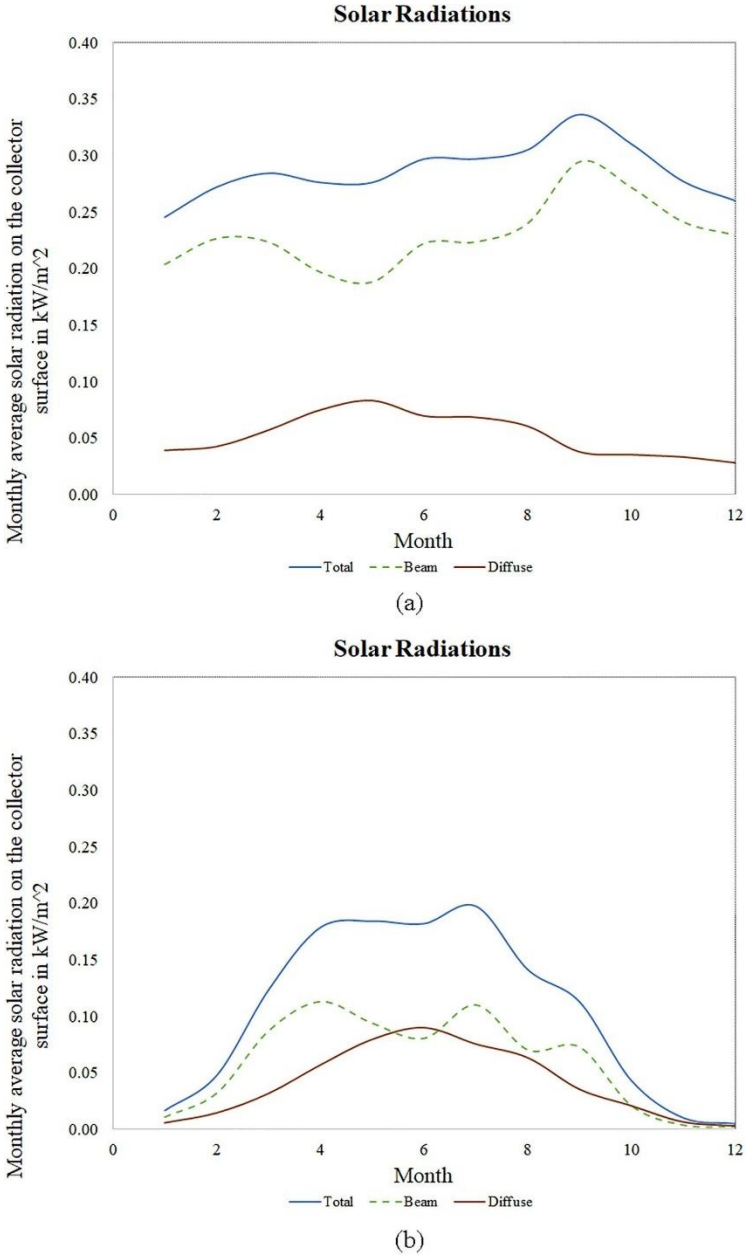

Fig. 8. Monthly Average Total, Beam and Diffuse Solar Radiations (a) for Zahedan (b) for Kingisepp.

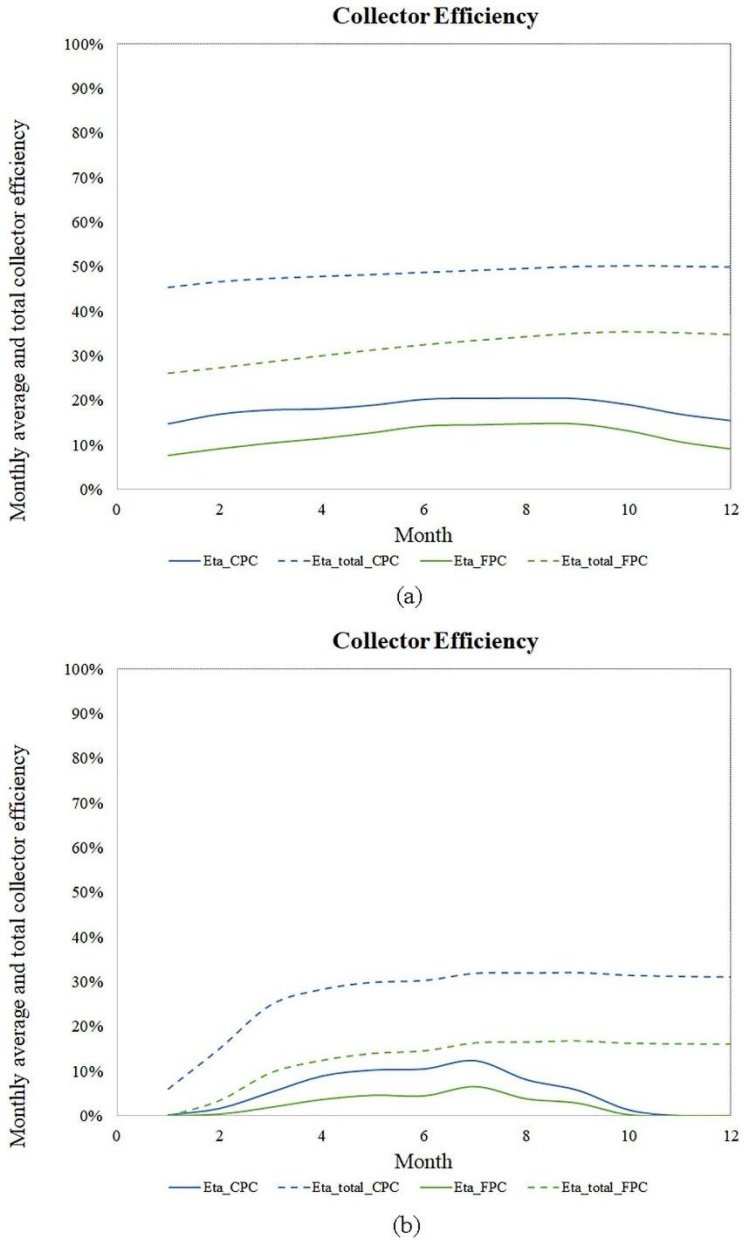

Fig. 9. Monthly Average and Total Collector Efficiencies (a) for Zahedan (b) for Kingisepp.

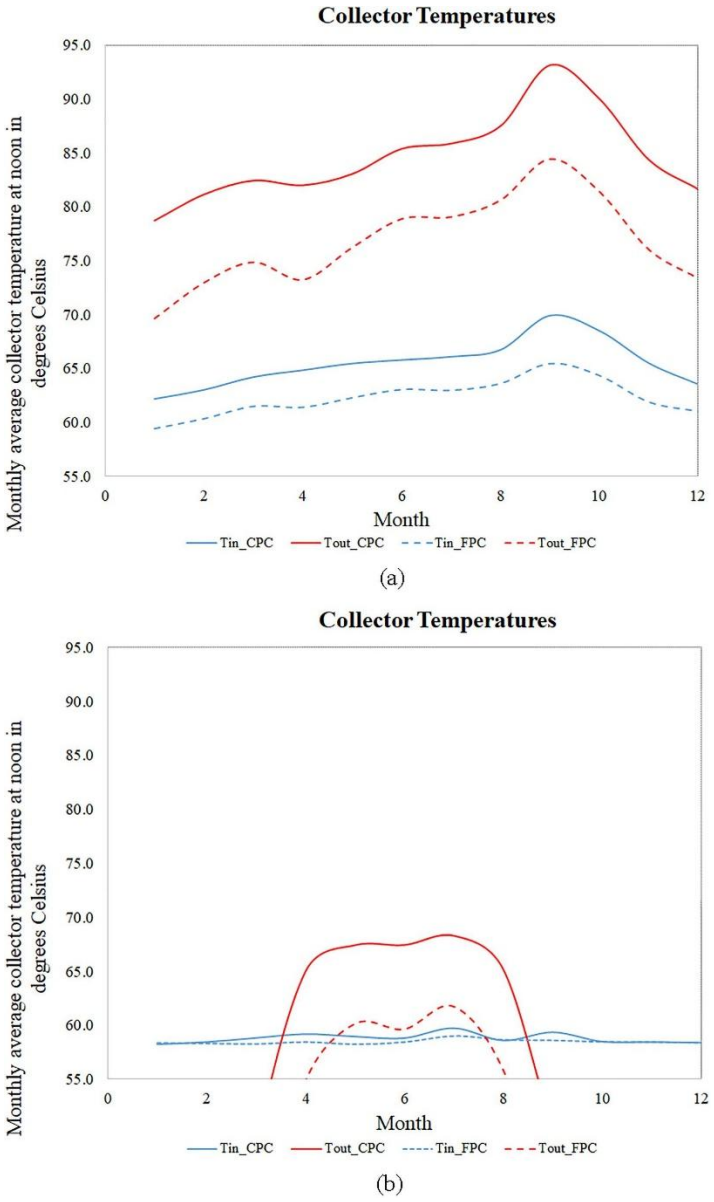

Fig. 10. Monthly Average Collector Temperatures at Noon (a) for Zahedan (b) for Kingisepp.

Fig. 11 compares the storage tank's hourly average temperatures. The dead band temperature deference of 5 °C allows the tank temperature to deviate from the setpoint temperature of 60 °C no more than 5 °C. Throughout the year, CPC provides higher tank temperatures in both locations, which is desirable for the end-user, meaning that less auxiliary energy should be purchased for water heating. However, due to low radiations, the storage tank has a very lower temperature in Kingisepp. The hourly average collector's useful solar heat gain and the system's auxiliary heating rates are shown in Fig. 12.

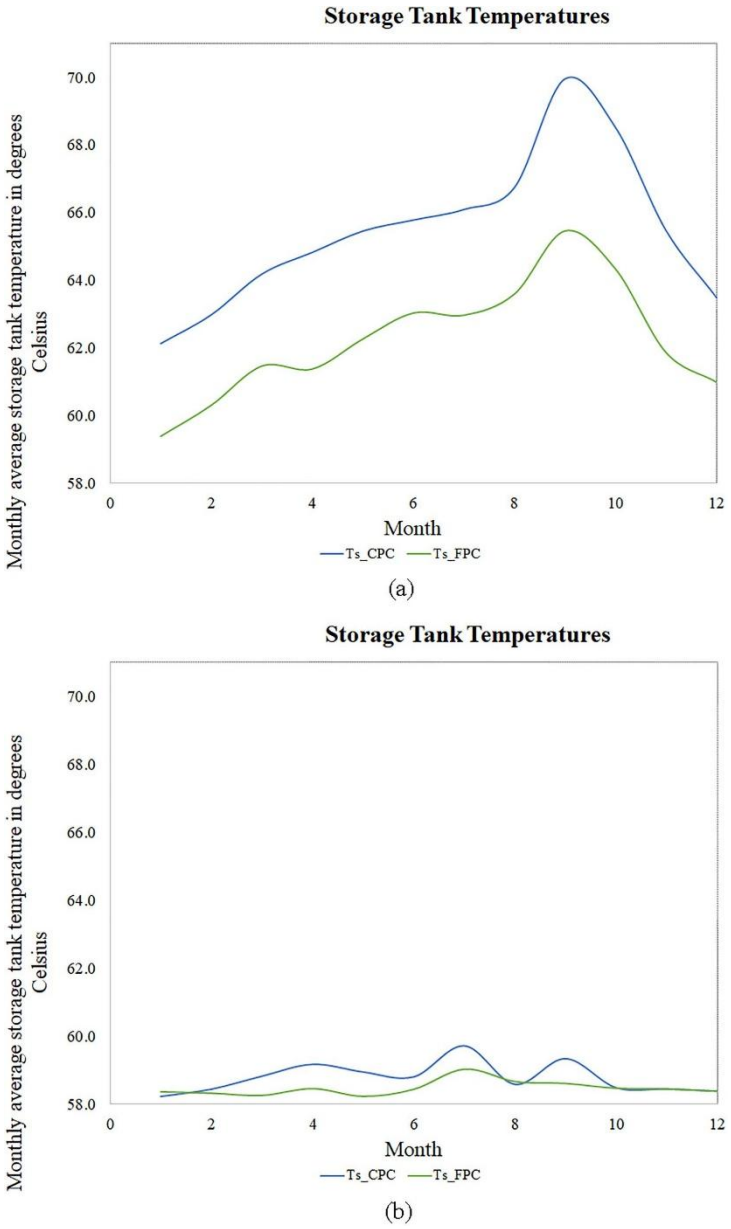

Fig. 11. Monthly Average Storage Tank Temperatures (a) for Zahedan (b) for Kingisepp.

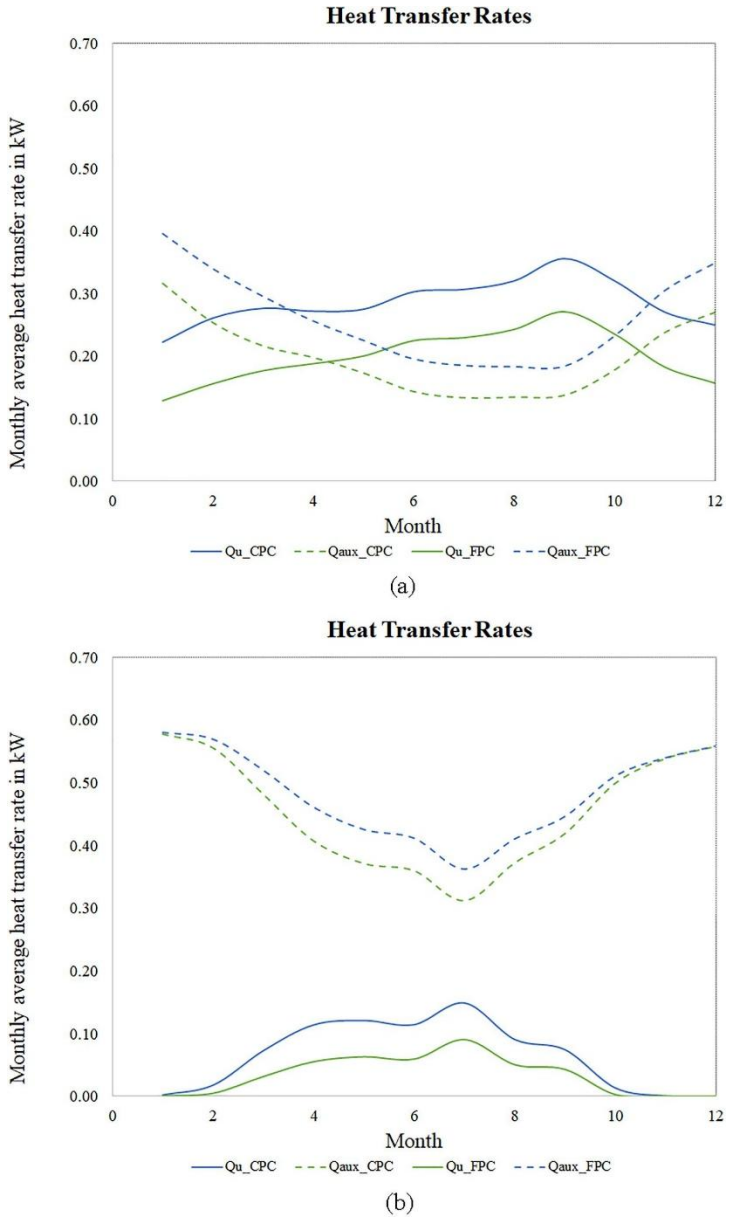

Fig. 12. Monthly Average Useful Heat Gains Q_u and Auxiliary Heating Rates Q_{aux} (a) for Zahedan (b) for Kingisepp.

Collecting more useful solar heat gain by the CPC is evident in both selected locations. Moreover, it can be seen that in both locations utilizing the CPC lowers the average monthly auxiliary power consumption in all months. In other words, in both locations, utilizing the CPC would cut down the auxiliary power requirements of the system compared with the situation that the FPC is used. This observation is of economic and environmental importance. Another important observation is that, in both cities, the CPC provides auxiliary power savings in both yearly and seasonal periods. It means that for either seasonal hot water demands like space heating or perennial demands like domestic hot water, CPC could be used to cut down the auxiliary power requirements.

Table 5, Table 6 summarize yearly useful solar energy gains, collector efficiencies, and required auxiliary energies of CPC and flat plate collector, for Zahedan and Kingisepp,

discussed above. In both cities, CPC collects more useful solar heat gain, which results in less auxiliary power requirement. In Zahedan, the energy-saving of CPC is much more impactful.

Table 5. Yearly results for Zahedan.

Collector	Useful solar energy gain [kWh]	Collector efficiency [–]	Required auxiliary energy [kWh]	% of auxiliary energy saving of CPC
CPC	2,510	0.5	1,740	24%
FPC	1,747	0.35	2,297	

Table 6. Yearly results for Kingisepp.

Collector	Useful solar energy gain[kWh]	Collector efficiency [-]	Required auxiliary energy [kWh]	% of auxiliary energy saving of CPC
CPC	563	0.31	3,981	6%
FPC	292	0.16	4,227	

In Table 7, yearly useful solar heat gains, efficiencies, and auxiliary heating rates for both collectors alongside the electricity prices for locations with the highest radiation-highest price, highest radiation-lowest price, lowest radiation-highest price, and lowest radiation-lowest price in latitudes of 0, 15, 30, 45 and 60° of the northern hemisphere are presented. Yearly total solar radiations on the collector's surface in selected locations range from 2,509 kWh/m^2 in Zahedan in Iran to 852 kWh/m^2 in Chongqing/Chungking in China. Also, electricity cost varies between 0.28 USD/kWh in Japan to 0.01 USD/kWh in Iran. In each latitude, the four selected locations present the locations with the highest radiation-highest price, highest radiation-lowest price, lowest radiation-highest price, and lowest radiation-lowest price (Fig. 7). The last column shows the saving in yearly auxiliary power consumption of the system if the flat plate collector is replaced with the CPC. It is seen that CPC keeps its advantage over flat plate collectors in all locations. It is interesting to notice that in locations with high solar radiation like Shambat, Ovda and Zahedan the auxiliary power savings are much more significant compared with locations like Kingisepp, Malung, and Chongqing/Chungking with low amounts of yearly available solar radiations. Fig. 13 compares the percentage of auxiliary power saving with total solar radiation striking the collector's surface. It can be observed that in locations with the highest amount of total solar radiation, the electricity-saving of the system with CPC is most considerable, and the effect of CPC in energy-saving becomes insignificant in low radiation sites, the same observation made in comparing collectors in Zahedan and Kingisepp as well. In the next section, a feasibility study regarding the costs and savings of using CPC instead of FPC will be provided.

Table 7. Yearly performance of collectors.

Latitude [oN]	Location	Country	Electricity price [USD/kWh] [47]	IT [kWh/m^2]	Ratio of diffuse to total radiation [–]	Collector	Qu [kWh]	Eta [–]	Qaux [kWh]	% of auxiliary energy saving of CPC	Saving of CPC in Qaux [kWh]
0	Garissa	Kenya	0.22	2161	0.41	CPC	2137	49%	1683	23%	498
						FPC	1473	34%	2181		
	Otavalo	Ecuador	0.1	2055	0.40	CPC	1752	43%	2584	18%	584
						FPC	1053	26%	3168		
	Makokou	Gabon	0.21	1648	0.55	CPC	1401	43%	2443	15%	440
						FPC	876	27%	2883		
	Kuching	Malaysia	0.06	1519	0.61	CPC	1265	42%	2471	12%	341
						FPC	847	28%	2811		
15	Hombori	Mali	0.22	2265	0.47	CPC	2285	50%	1544	22%	441
						FPC	1678	37%	1985		
	Shambat	Sudan	0.04	2471	0.31	CPC	2604	53%	1265	27%	470
						FPC	1909	39%	1735		
	Guatemala	Guatmala	0.25	1942	0.41	CPC	1713	44%	2390	20%	598
						FPC	998	26%	2988		
	Nellore	India	0.08	1840	0.51	CPC	1739	47%	1946	15%	343
						FPC	1307	36%	2289		
30	Ovda	Israel	0.17	2373	0.21	CPC	2355	50%	1829	24%	579
						FPC	1604	34%	2408		
	Zahedan	Iran	0.01	2509	0.18	CPC	2510	50%	1740	24%	557
						FPC	1747	35%	2297		
	Amite LA	US	0.15	1707	0.42	CPC	1497	44%	2555	15%	456
						FPC	957	28%	3011		
	Chongqing	China	0.08	852	0.74	CPC	517	30%	3484	5%	189
						FPC	303	18%	3673		

Latitude [oN]	Location	Country	Electricity price [USD/kWh] [47]	IT [kWh/m^2]	Ratio of diffuse to total radiation [–]	Collector	Qu [kWh]	Eta [–]	Qaux [kWh]	% of auxiliary energy saving of CPC	Saving of CPC in Qaux [kWh]
45	Torino	Italy	0.27	1494	0.34	CPC	1178	39%	3138	11%	389
						FPC	722	24%	3527		
	Sainshand	Mongolia	0.04	2207	0.19	CPC	1937	44%	2808	21%	757
						FPC	1033	23%	3564		
	Wakkanai	Japan	0.28	1185	0.47	CPC	750	32%	3745	10%	408
						FPC	317	13%	4153		
	Banja Luka	Bosnia	0.1	1221	0.44	CPC	887	36%	3414	8%	313
						FPC	539	22%	3727		
	Russaro	Finland	0.19	1012	0.35	CPC	648	32%	3858	9%	376
						FPC	237	12%	4233		
	Kingisepp	Russia	0.06	908	0.39	CPC	563	31%	3981	6%	247
						FPC	292	16%	4227		
60	Malung	Sweden	0.19	974	0.34	CPC	598	31%	4022	6%	266
						FPC	308	16%	4289		
	Ust-Maja	Russia	0.06	1515	0.21	CPC	1026	34%	4208	10%	447
						FPC	528	17%	4655		

[1]For each latitude, the four selected locations represent the locations with the highest radiation-highest price, highest radiation-lowest price, lowest radiation-highest price, and lowest radiation-lowest price, respectively (Fig. 7 and Table 8).

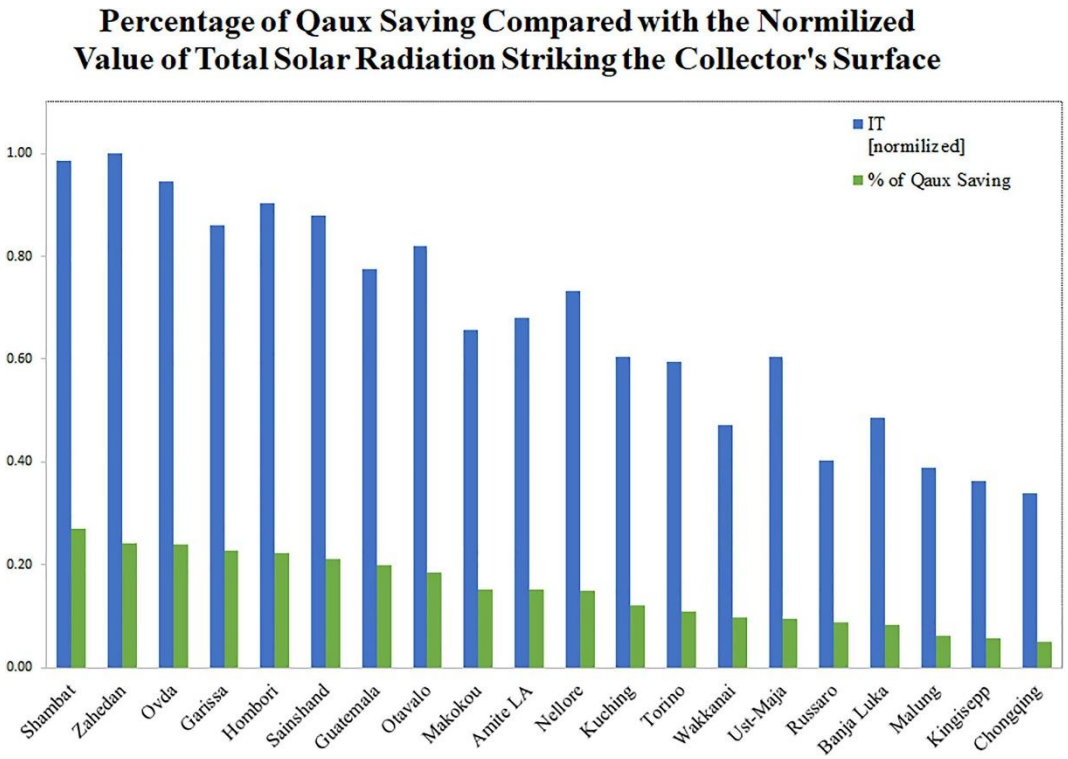

Fig. 13. Comparing the Percentage of Auxiliary Power Saving with the Normalized Value of Total Solar Radiation Striking the Collector's Surface.

5.2. Life cycle cost analysis

In this section, the aim is to examine whether the energy savings of CPC justify the extra investment required for its purchase. Unlike flat plate collectors, not so many collector manufactures produce CPC. The authors acquired the collector prices from a manufacturer in Europe that manufactures both CPC and flat plate collectors [48]. The collectors have equal weights and aperture areas. The manufacturer offers two series of flat plate collectors, high-price and low-price flat plate collectors, allowing the authors to compare the feasibility of using CPC instead of flat plate collectors with different costs. The CPC, high-price, and low-price flat plate collectors cost 1,195, 960, and 725 USD, respectively.

For the economic analysis, the well known Net-Present Value (NPV) method is used. In this section, the life cycle cost analysis (LCCA) method is used to investigate the economic profitability of the investment on a CPC collector. A review and description of the LCCA method can be found in [49], [50], [51]. The Net-Present Value (NPV) is calculated as:

$$NPV = \sum_{t=1}^{n} \frac{R_t}{(1+i)^t} \tag{28}$$

where R_t, i, and represent the net cash inflow-outflows during a single period, discount rate or return that could be earned in alternative investment, and the number of periods, respectively. NPV could be defined as today's value of the expected cash flows minus today's value of invested cash. In this project, the aim is to invest some extra money to purchase CPC and save electricity cost in return. Therefore, the investment is the difference

between the CPC and flat plate collector prices:Investment = CPC price flat plate collector prices:

$$\text{Investment } [USD] = \text{CPC price } [USD] - \text{flat plate collector price} [USD]$$

The saving of this investment is also the cost of auxiliary power saved by the CPC with respect to the FPC:

$$\text{Investment saving } [USD] = \text{auxiliary power saved by the CPC with respect to the FPC } [kWh] \times \text{electricity cost } [USD/kWh]$$

Table 8 presents the net present value (NPV), saving to investment ratio (SIR), and a simple payback period of a 20-year investment for utilizing a CPC in the water heating system. The study is carried out in two scenarios. In scenario-I and scenario-II, the CPC is compared with the low and the high-price flat plate collectors, respectively. In all latitudes, in locations with the highest electricity price, CPC in both scenarios is feasible regardless of solar radiation availability. Also, in all latitudes, the CPC investment in the locations with the lowest radiation and lowest price in scenario-I is not feasible. However, except for Ust-Maja in Russia, in all other cases still scenario-II, replacing a high price flat plate collector with CPC could be justifiable economically, though with very insignificant returns. For both scenarios, in Russia, due to low solar radiation, very low electricity costs, and high discount rates, investment in CPC is not profitable. For all locations, except for Iran and Russia, with very low energy prices and high discount rates, replacing a high price flat plate collector with CPC can be justified. Fig. 14 compares NPV with electricity prices. Maximum NPVs are all achieved in the locations with the highest electricity prices, and it is seen that the decrease in electricity price affects the feasibility of CPC adversely. According to Fig. 15, the highest NPVs are achieved in locations with the lowest discount rates. Fig. 16 compares NPV with total solar radiation striking the collector's surface. No direct or meaningful relation between available solar energy and profitability of CPC is observed. In other words, the impact of solar radiation on the profitability of CPC is not decisive. The key observation is that in locations with high electricity prices and not very much discount rates, even in case of relatively low solar radiation, investment in CPC would yield the highest profits.

Table 8. Feasibility of utilization of CPC.

Latitude [°N]	Location	Country	Radiation-cost combination	Electricity price [USD/kWh] [47]	Discount rate [-] [52]	Saving of CPC in Qaux [kWh]	Saving of CPC in Qaux [USD]	Scenario- I			Scenario- II		
								Net present value [USD]	Saving to investment ratio [-]	Simple payback period [years]	Net present value [USD]	Saving to investment ratio [-]	Simple payback period [years]
0	Garissa	Kenya	highest radiation -highest price	0.22	10.00	498	109.64	463	2	4.3	698	4	2.1
	Otavalo	Ecuador	highest radiation-lowest price	0.1	8.17	584	58.44	97	1.2	8	332	2.4	4
	Makokou	Gabon	lowest radiation-highest price	0.21	3.00	440	92.39	905	2.9	5.1	1140	5.8	2.5
	Kuching	Malaysia	lowest radiation-lowest price	0.06	3.00	341	20.43	−166	0.6	23	69	1.3	11.5
15	Hombori	Mali	highest radiation -highest price	0.22	16.00	441	97.09	106	1.2	4.8	341	2.4	2.4
	Shambat	Sudan	highest radiation-lowest price	0.04	Not Available	470	18.79	–	–	–	–	–	–
	Guatemala	Guatmala	lowest radiation-highest price	0.25	7.53	598	149.48	1050	3.2	3.1	1285	6.5	1.6
	Nellore	India	lowest radiation-lowest price	0.08	6.00	343	27.47	−155	0.7	17.1	80	1.3	8.6

Latitude [°N]	Location	Country	Radiation-cost combination	Electricity price [USD/kWh] [47]	Discount rate [-] [52]	Saving of CPC in Qaux [kWh]	Saving of CPC in Qaux [USD]	Scenario- I			Scenario- II		
								Net present value [USD]	Saving to investment ratio [-]	Simple payback period [years]	Net present value [USD]	Saving to investment ratio [-]	Simple payback period [years]
30	Ovda	Israel	highest radiation -highest price	0.17	0.10	579	98.44	1478	4.1	4.8	1713	8.3	2.4
	Zahedan	Iran	highest radiation-lowest price	0.01	15.00	557	5.57	−435	0.1	84.4	−200	0.1	42.2
	Amite LA	US	lowest radiation-highest price	0.15	0.50	456	68.34	828	2.8	6.9	1063	5.5	3.4
	Chongqing	China	lowest radiation-lowest price	0.08	2.25	189	15.15	−228	0.5	31	7	1	15.5
45	Torino	Italy	highest radiation -highest price	0.27	0.25	389	104.99	1576	4.4	4.5	1811	8.7	2.2
	Sainshand	Mongolia	highest radiation-lowest price	0.04	11.00	757	30.27	−229	0.5	15.5	6	1	7.8
	Wakkanai	Japan	lowest radiation-highest price	0.28	0.30	408	114.34	1746	4.7	4.1	1981	9.4	2.1
	Banja Luka	Bosnia	lowest radiation-lowest price	0.1	Not Available	313	31.33	–	–	–	–	–	–
60	Russaro	Finland	highest radiation -highest price	0.19	1.25	376	71.39	786	2.7	6.6	1021	5.3	3.3

Latitude [°N]	Location	Country	Radiation-cost combination	Electricity price [USD/kWh] [47]	Discount rate [-] [52]	Saving of CPC in Qaux [kWh]	Saving of CPC in Qaux [USD]	Scenario- I			Scenario- II		
								Net present value [USD]	Saving to investment ratio [-]	Simple payback period [years]	Net present value [USD]	Saving to investment ratio [-]	Simple payback period [years]
	Kingisepp	Russia	highest radiation-lowest price	0.06	10.00	247	14.79	−344	0.3	31.8	−109	0.5	15.9
	Malung	Sweden	lowest radiation-highest price	0.19	−0.50	266	50.57	597	2.3	9.3	832	4.5	4.6
	Ust-Maja	Russia	lowest radiation-lowest price	0.06	10.00	447	26.82	−242	0.5	17.5	−7	1	8.8

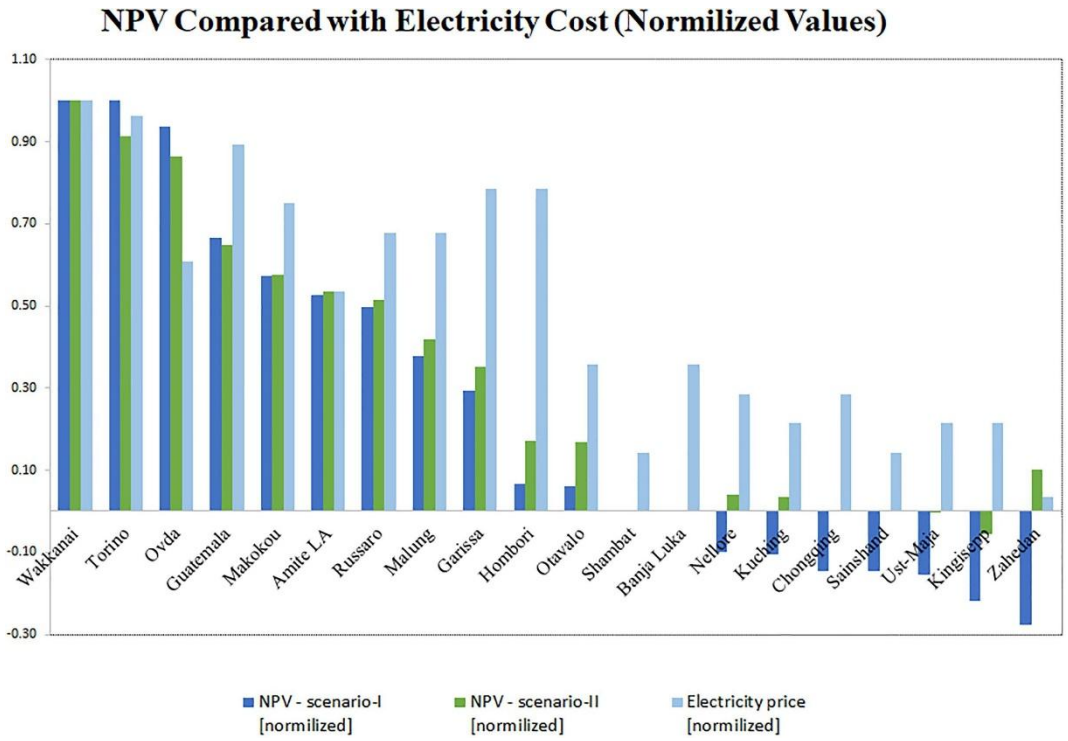

Fig. 14. Comparing NPV with Electricity Cost (Normalized Values).

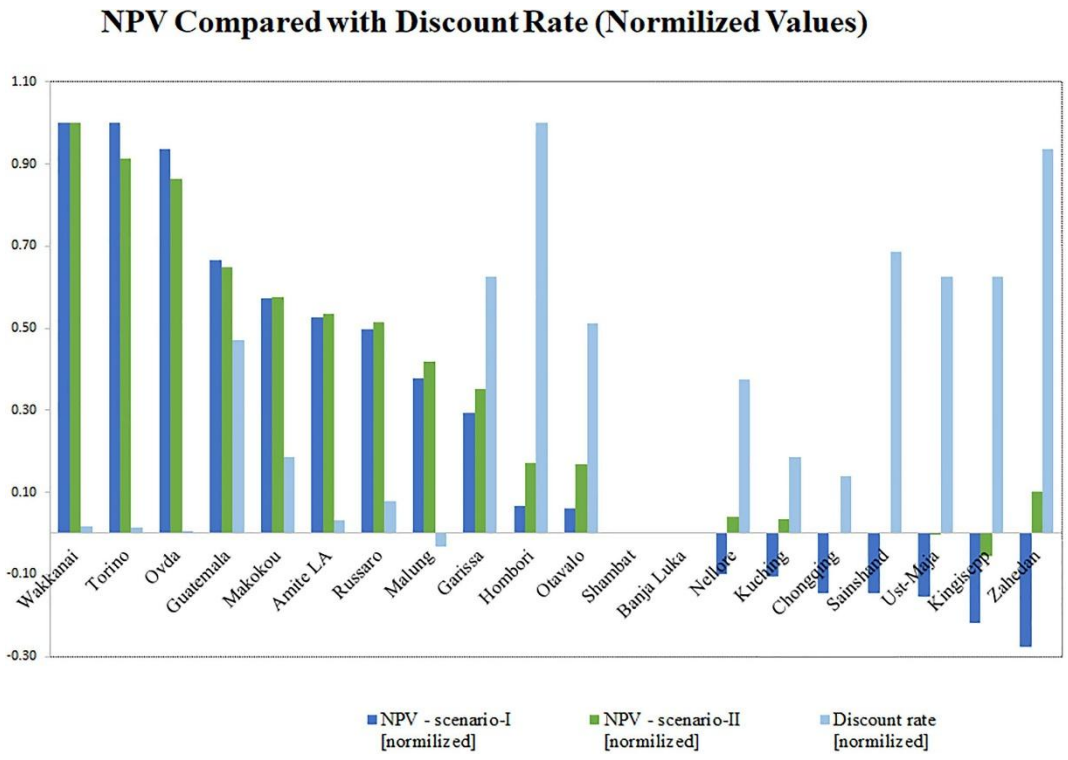

Fig. 15. Comparing NPV with Discount Rate (Normalized Values).

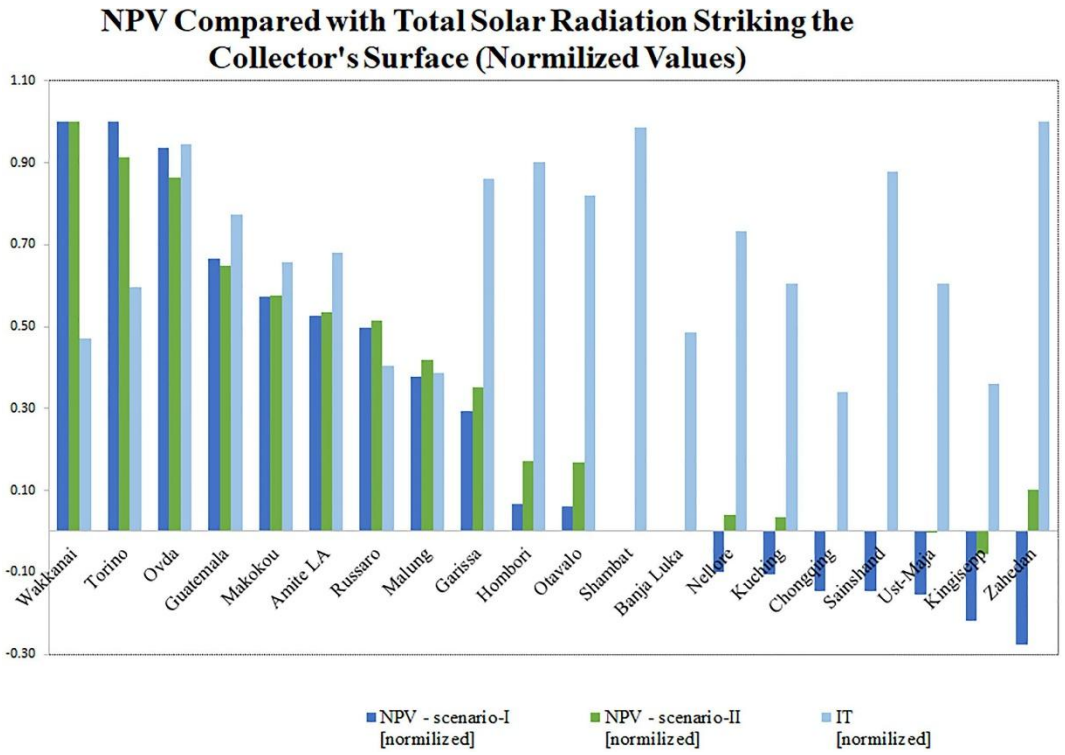

Fig. 16. Comparing NPV with Total Solar Radiation Striking the Collector's Surface (Normalized Values).

6. Conclusion

No solar heating system can operate entirely by solar radiation and incorporating an auxiliary energy source for the conditions that enough solar energy is not available is ineluctable. This study indicates that in all selected locations with high and low solar radiation, utilizing a CPC could increase the yearly useful solar heat gain from 214 kWh in China to 904 kWh in Mongolia. Consequently, the annual demand for auxiliary power for water heating demand would be lowered from 189 kWh in China to 757 kWh in Mongolia. Results show that in the locations with the highest solar radiation availability, the energy-saving of CPC is enhanced. As the global solar radiation declines, the energy-saving of CPC becomes less substantial. A feasibility study on the studied locations implies that, regardless of solar radiation availability, investment in CPC is feasible in locations with the highest electricity prices. In Kenya, Gabon, Mali, Guatemala, Israel, USA, Italy, Japan, Finland, and Sweden, the locations in the selected latitudes with the highest electricity prices from 0.15 to 0.28 USD/kWh, investment in CPC for water heating is supported by economical analysis and NPV of a 20-year investment ranges from 341 to 1,981 USD. Among these locations, NPV of investment on CPC in Gabon, Guatemala, USA, Japan and Sweden with low levels of solar radiation between 974 and 1,942 kWh/m^2, is between 832 and 1,981 USD at the end of the project's life time and justifies the employment of this type of solar collector in sites with high energy prices, even though not much solar radiation is available. Maximum NPVs are all achieved in locations with the highest electricity prices and lowest discount rates, even in relatively low solar radiation cases. Selected locations in Japan and Italy with maximum NPV values of 1,981 and 1,811 UDS, respectively, have the highest electricity rates of 0.28 and 0.27 USD/kWh, in respect. In both countries, the discount rate is relatively low and about 0.3. So, in locations that energy price is a concern, and renewable energies are common, CPC has a good chance to save money for the end-user. In other words, in locations where flat plate

collectors are already being used, replacing them with CPC could cut the auxiliary power requirements, which in the long run, could result in considerable cost savings and CO2 reductions. CPC's potential advantages over flat plate collectors for solar water heating systems could be a subject for more extensive numerical and experimental studies.

Declaration of Competing Interest

The author declare that there is no conflict of interest.

References

[1] C. Hsieh. Thermal analysis of CPC collectors. Solar Energy, 27 (1) (1981), pp. 19-29

[2] R. Winston.Principles of solar concentrators of a novel design. Sol. Energy, 16 (2) (1974), pp. 89-95

[3] A.-E.-A. Cairo, J.A. Clark. A thermal-optical analysis of a compound parabolic concentrator for single and multiphase flows, including superheat. Wärme-und Stoffübertragung, 21 (2–3) (1987), pp. 189-198

[4] S. Chakraverty, N. Bansal, H. Garg. Transient analysis of a CPC collector with time dependent input function. Sol. Energy, 38 (3) (1987), pp. 179-185

[5] R. Tchinda, E. Kaptouom, D. Njomo. Study of the CPC collector thermal behaviour. Energy Convers. Manage., 39 (13) (1998), pp. 1395-1406

[6] N. Fraidenraich, R.D.C. De Lima, C. Tiba, E.d.S. Barbosa, Simulation model of a CPC collector with temperature-dependent heat loss coefficient, Solar energy 65(2) (1999) 99-110.

[7] R. Oommen, S. Jayaraman. Development and performance analysis of compound parabolic solar concentrators with reduced gap losses—‘V’groove reflector. Renew. Energy, 27 (2) (2002), pp. 259-275

[8] M. Collares-Pereira, M. Carvalho, J. de Oliveira. New low concentration CPC type collector with convection controlled by a honeycomb TIM material: a compromise with stagnation temperature control and survival of cheap fabrication materials, Proceedings of the ISES 2003 Solar World Congress, Göteborg, Sweden, 2003.

[9] Y. Tripanagnostopoulos, P. Yianoulis, S. Papaefthimiou, S. Zafeiratos. CPC solar collectors with flat bifacial absorbers. Sol. Energy, 69 (3) (2000), pp. 191-203

[10] M. Adsten, B. Hellström, B. Karlsson. Measurement of radiation distribution on the absorber in an asymmetric CPC collector. Sol. Energy, 76 (1–3) (2004), pp. 199-206

[11] P. Eames, M. Smyth, B. Norton. The experimental validation of a comprehensive unified model for optics and heat transfer in line-axis solar energy systems Sol. Energy, 71 (2) (2001), pp. 121-133

[12] Y. Fang, P.C. Eames, T.J. Hyde, B. Norton. Thermal performance of complex multimaterial frames for evacuated glazing, ISES solar world congress, 14th to 19th June, 2003.

[13] T. Mallick, P. Eames, T. Hyde, B. Norton. The design and experimental characterisation of an asymmetric compound parabolic photovoltaic concentrator for building façade integration in the UK. Sol. Energy, 77 (3) (2004), pp. 319-327

[14] M. Carvalho, M. Collares-Pereira, J. Gordon, A. Rabl. Truncation of CPC solar collectors and its effect on energy collection. Sol. Energy, 35 (5) (1985), pp. 393-399

[15] J. Gordon. Ideal solar concentrators for photoelectrochemical cells. Sol. Energy, 40 (4) (1988), pp. 391-395

[16] A. Sohani, S. Hoseinzadeh, K. Berenjkar. Experimental analysis of innovative designs for solar still desalination technologies; an in-depth technical and economic assessment. J. Storage Mater. (2020), Article 101862

[17] S. Hoseinzadeh, A. Sohani, S. Samiezadeh, H. Kariman, M. Ghasemi. Using computational fluid dynamics for different alternatives water flow path in a thermal photovoltaic (PVT) system. Int. J. Numer. Meth. Heat Fluid Flow (2020)

[18] A. Sohani, H. Sayyaadi. Employing genetic programming to find the best correlation to predict temperature of solar photovoltaic panels Energy Convers. Manage., 224 (2020), Article 113291

[19] A. Sohani, H. Sayyaadi. Providing an accurate method for obtaining the efficiency of a photovoltaic solar module. Renew. Energy (2020)

[20] J. Varghese, K. Manjunath. A parametric study of a concentrating integral storage solar water heater for domestic uses. Appl. Therm. Eng., 111 (2017), pp. 734-744

[21] E. Chiavazzo, M. Morciano, F. Viglino, M. Fasano, P. Asinari. Passive solar high-yield seawater desalination by modular and low-cost distillation. Nat. Sustainability, 1 (12) (2018), pp. 763-772

[22] M. Rönnelid, B. Perers, B. Karlsson. Construction and testing of a large-area CPC-collector and comparison with a flat plate collector. Sol. Energy, 57 (3) (1996), pp. 177-184

[23] M. Jradi, S. Riffat. Medium temperature concentrators for solar thermal applications. Int. J. Low-Carbon Technol., 9 (3) (2012), pp. 214-224

[24] W.T. Welford, R. Winston. Optics of nonimaging concentrators. Light Solar Energy (1978)

[25] H. Baig, N. Sellami, D. Chemisana, J. Rosell, T.K. Mallick. Performance analysis of a dielectric based 3D building integrated concentrating photovoltaic system. Sol. Energy, 103 (2014), pp. 525-540

[26] H. Baig, N. Sarmah, D. Chemisana, J. Rosell, T.K. Mallick. Enhancing performance of a linear dielectric based concentrating photovoltaic system using a reflective film along the edge. Energy, 73 (2014), pp. 177-191

[27] G. Walze, P. Nitz, J. Ell, A. Georg, A. Gombert, W. Hossfeld. Combination of microstructures and optically functional coatings for solar control glazing. Sol. Energy Mater. Sol. Cells, 89 (2–3) (2005), pp. 233-248

[28] G.E. Arnaoutakis, J. Marques-Hueso, A. Ivaturi, S. Fischer, J.C. Goldschmidt, K.W. Krämer, B.S. Richards. Enhanced energy conversion of up-conversion solar cells by the integration of compound parabolic concentrating optics. Sol. Energy Mater. Sol. Cells, 140 (2015), pp. 217-223

[29] A. Al-Ghasem, G. Tashtoush, M. Aladeemy. Experimental study of tracking 2-D Compound Parabolic Concentrator (CPC) with flat plate absorber, Renewable Energy Research and Applications (ICRERA), 2013 International Conference on, IEEE, 2013, pp. 779-782.

[30] R. Mishra, V. Garg, G. Tiwari. Energy matrices of U-shaped evacuated tubular collector (ETC) integrated with compound parabolic concentrator (CPC), Solar Energy 153 (2017) 531-539.

[31] W. Ratismith, A. Inthongkhum, J. Briggs. Two non-tracking solar collectors: design criteria and performance analysis. Appl. Energy, 131 (2014), pp. 201-210

[32] B. Abdullahi, R. Al-Dadah, S. Mouhmud. Optical performance of double receiver compound parabolic concentrator. Energy Procedia, 61 (2014), pp. 2625-2628

[33] B. Abdullahi, R. Al-Dadah, S. Mahmoud, R. Hood. Optical and thermal performance of double receiver compound parabolic concentrator. Appl. Energy, 159 (2015), pp. 1-10

[34] M.R. Islam, K. Sumathy, S.U. Khan. Solar water heating systems and their market trends. Renew. Sustain. Energy Rev., 17 (2013), pp. 1-25

[35] M. Souliotis, Y. Tripanagnostopoulos. Study of the distribution of the absorbed solar radiation on the performance of a CPC-type ICS water heater. Renew. Energy, 33 (5) (2008), pp. 846-858

[36] M. Smyth, G. Barone, A. Buonomano, C. Forzano, G.F. Giuzio, A. Palombo, J. Mondol, R. Muhumuza, A. Pugsley, A. Zacharopoulos. Modelling and experimental evaluation of an innovative Integrated Collector Storage Solar Water Heating (ICSSWH) prototype. Renewable Energy (2020)

[37] L. Brottier, R. Bennacer. Thermal performance analysis of 28 PVT solar domestic hot water installations in Western Europe. Renew. Energy, 160 (2020), pp. 196-210

[38] P. Gang, L. Guiqiang, Z. Xi, J. Jie, S. Yuehong. Experimental study and exergetic analysis of a CPC-type solar water heater system using higher-temperature circulation in winter. Sol. Energy, 86 (5) (2012), pp. 1280-1286

[39] K. Devanarayanan, K.K. Murugavel. **Integrated collector storage solar water heater with compound parabolic concentrator–development and progress.** Renew. Sustain. Energy Rev., 39 (2014), pp. 51-64

[40] Y. Tripanagnostopoulos, M. Souliotis. **ICS solar systems with horizontal cylindrical storage tank and reflector of CPC or involute geometry.** Renewable Energy, 29 (1) (2004), pp. 13-38

[41] J.-J. Ning, Y.-Z. Zhu, H.-J. Chen, Y. Wang, D.-D. Guo, J.-Z. Jiang, C.-H. Liao. **Experimental study of a novel CPC heat pipe coupled vacuum tube solar water heater [J].** Vacuum, 4 (2012)

[42] J. Varghese, Samsher, K. Manjunath. Techno-economic analysis of an integrated collector storage solar water heater with CPC reflector for households. International Journal of Ambient Energy 39(8) (2018) 885–890.

[43] L. University of Wisconsin--Madison. Solar Energy, TRNSYS, a transient simulation program, Madison, Wis. : The Laboratory, 1975.1975.

[44] J.A. Duffie, W.A. Beckman. **Solar Engineering of Thermal Processes.** John Wiley & Sons (2013)

[45] S.A. Klein. **A design procedure for solar heating systems, chemical engineering.** The University of Winsconsin-Madison (1976)

[46] A. Rabl. **Optical and thermal properties of compound parabolic concentrators.** Sol. Energy, 18 (6) (1976), pp. 497-511

[47] GlobalPetrolPrices, Electricity prices. https://www.globalpetrolprices.com/electricity_prices/. (Accessed June 2020).

[48] SOLARFOCUS. https://www.solarfocus.com/en. (Accessed June 2020).

[49] C.O. Okoye, B.C. Oranekwu-Okoye. **Economic feasibility of solar PV system for rural electrification in Sub-Sahara Africa.** Renew. Sustain. Energy Rev., 82 (2018), pp. 2537-2547

[50] C.O. Okoye, O. Solyalı. **Optimal sizing of stand-alone photovoltaic systems in residential buildings.** Energy, 126 (2017), pp. 573-584

[51] C.O. Okoye, O. Taylan, D.K. Baker. **Solar energy potentials in strategically located cities in Nigeria: Review, resource assessment and PV system design.** Renew. Sustain. Energy Rev., 55 (2016), pp. 550-566

[52] Photius, Central bank discount rate (%) 2019 Country Ranks, by Rank. https://photius.com/rankings/2019/economy/central_bank_discount_rate_2019_0.html. (Accessed June 2020).